Loss of mitogen-activated protein kinase kinase kinase 4 (MEKK4) results in enhanced apoptosis and defective neural tube development

Hongbo Chi*†, Matthew R. Sarkisian†‡, Pasko Rakic‡, and Richard A. Flavell*§¶

*Section of Immunobiology, ‡Department of Neurobiology and Kavli Institute of Neuroscience, and §Howard Hughes Medical Institute, Yale University School of Medicine, New Haven, CT 06520

Contributed by Richard A. Flavell, January 3, 2005

Neural tube defects (NTDs) are prevalent human birth defects. Mitogen-activated protein kinases (MAPKs), such as c-Jun N-terminal kinase (JNK), are implicated in facilitating neural tube closure, yet upstream regulators remain to be identified. Here, we show that MAP kinase kinase kinase 4 (MEKK4) is strongly expressed in the developing neuroepithelium. Mice deficient in MEKK4 develop highly penetrant NTDs that cannot be rescued by supplementation with folic acid or inositol. Unlike most mouse models of NTDs, MEKK4 mutant embryos display genetically cosegregated exencephaly and spina bifida, recapitulating the phenotypes observed in human patients. To identify downstream targets of MEKK4 during neural tube development, we examined the activity of MAP kinase kinase 4 (MKK4), a signaling intermediate between MAP kinase kinase kinase and JNK/p38. We found a significant reduction in MKK4 activity in MEKK4-deficient neuroepithelium at sites of neural tube closure. MAPK pathways are key regulators of cell apoptosis and proliferation. Analyses of the neuroepithelium in MEKK4-deficient embryos showed massively elevated apoptosis before and during neural tube closure, suggesting an antiapoptotic role for MEKK4 during development. In contrast, proliferation of MEKK4-deficient neuroepithelial cells appeared to be largely unaffected. MEKK4 therefore plays a critical role in regulating MKK4 activity and apoptotic cell death during neural tube development. Disruption of this signaling pathway may be clinically relevant to folate-resistant human NTDs.

exencephaly | folate | neurulation | spina bifida

Neural tube defects (NTDs), caused by unknown genetic predisposition in combination with unfavorable environmental conditions, are prevalent birth defects in humans (1). Direct genetic analysis of human NTDs has been difficult because of the scarcity of useful familial cases. Accordingly, no human genes associated with NTDs have been identified. Mutant mice are valuable systems to identify candidate genes for human NTDs, and to unravel the molecular mechanisms involved. These studies have revealed that NTDs can result from alterations in cell proliferation, cell survival, actin cytoskeletal regulation of the developing neuroepithelium, and patterning abnormalities that involve sonic hedgehog and planar cell polarity pathways (2, 3). Apoptotic cell death is present in the developing neuroepithelium, and dysregulation in this process is detrimental to neural tube development (2). Several mouse strains with mutations in apoptosis-related genes develop NTDs that are associated with changes in the extent of neuroepithelial cell death. For example, caspase-9-deficient embryos develop NTDs associated with reduced apoptosis (4, 5), whereas *Splotch* (Pax3 deficiency) mice display NTDs and excessive neuroepithelial cell death (6, 7). Thus, either decreased or increased apoptosis leads to NTDs, indicating a specific physiological role of neuroepithelial cell death during neural tube development.

Stress-activated MAP kinases (MAPKs), including p38 and c-Jun N-terminal kinase (JNK), are key regulators of apoptotic cell death. They exert pro- or antiapoptotic effects, depending on a particular cellular context (8, 9). This feature is exemplified by the alterations in the neuroepithelial cell death in mice deficient in both JNK1 and JNK2 genes that develop NTD and early embryonic lethality. Specifically, there is a reduction in cell death in the lateral edges of hindbrain (HB) before neural tube closure. In contrast, increased apoptosis is prominent in the mutant forebrain (FB), leading to precocious degeneration (10, 11). Therefore, JNK genes regulate region-specific apoptosis during early brain development. Because JNK activity depends on coordinated signaling of MAP kinase kinases and MAP kinase kinase kinases (MAP3Ks) (8, 9), these upstream pathways would be predicted to play a role in modulating regional apoptosis during development. However, these pathways have yet to be identified.

Our laboratory has recently generated mice deficient in MAP kinase kinase kinase 4 (MEKK4), a MAP3K in the JNK/p38 pathway, to study the regulation of MAPK pathways in the immune system (12). Here, we report that MEKK4−/− mice on a C57BL/6 background develop NTDs associated with enhanced apoptosis in the developing neuroepithelium. We further show that activity of MAP kinase kinase 4 (MKK4, also known as SEK1), a signaling intermediate between MAP3K and JNK/p38 (13), is significantly reduced in MEKK4−/− neuroepithelium. Our results have identified a previously unappreciated function of the MEKK4 and MKK4 pathway in the regulation of apoptosis and neural tube development.

Methods

Mice and Treatment. The generation of MEKK4−/− mice on a mixed C57BL/6 × 129/SvE background has been described (12). In this study, MEKK4+/− mice were backcrossed onto C57BL/6 strain (National Cancer Institute, Frederick, MD) for six to nine generations and then intercrossed. Fetal stage was calculated from the day when a vaginal plug was observed [considered as embryonic day (E)0.5], and confirmed by comparing the morphology to characterized embryonic structures (14). To test the responsiveness of NTDs to nutrient supplementation, folic acid (Sigma, 25 mg/kg), myo-inositol (Calbiochem, 400 mg/kg), or PBS was administered by daily i.p. injection to pregnant MEKK4+/− females between gestational days 6.5 and 9.5 as described (15, 16). Embryos were collected between E14.5-E18.5, examined morphologically, and genotyped by PCR.

Abbreviations: NTD, neural tube defect; MAP, mitogen-activated protein; MAPK, MAP kinase; MEKK4, MAP kinase kinase kinase 4; MAP3K, MAP kinase kinase kinase; MKK4, MAP kinase kinase 4; JNK, c-Jun N-terminal kinase; PFA, paraformaldehyde; LT, lamina terminalis; FB, forebrain; HB, hindbrain; EX, exencephaly; SB, spina bifida; CT, curled tail; E*n*, embryonic day *n*.

†H.C. and M.R.S. contributed equally to this work.

¶To whom correspondence should be addressed. E-mail: richard.flavell@yale.edu.

www.pnas.org/cgi/doi/10.1073/pnas.0500026102

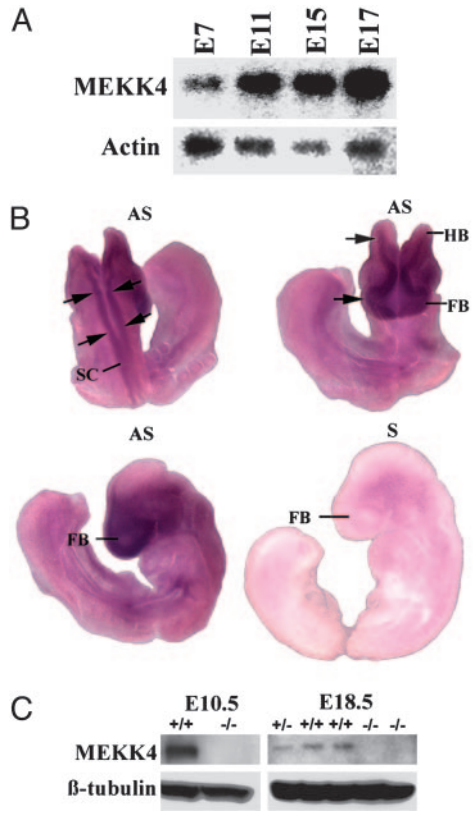

Fig. 1. MEKK4 expression during mouse development. (*A*) Northern blot analysis showed that MEKK4 mRNA is expressed in E7-E17 embryos. Actin was used as a loading control. (*B*) Whole-mount *in situ* hybridization for MEKK4 mRNA at E9. Three different views of the embryo surface are shown: dorsal view (*Left Upper*), anterior-horizontal view (*Right Upper*), and lateral view (*Lower*). Compared with the sense probe (S) control (*Right Lower*), the antisense (AS) probe revealed specific MEKK4 expression. More prominent signals were detected along the neuraxis, from the FB to HB regions and spanning the length of the spinal cord (SC). (*C*) Western blot analysis of E10.5 whole-head and E18.5 fetal-brain extracts showed that MEKK4−/− mice lack the expression of MEKK4 protein compared with MEKK4+/+ and MEKK4+/− mice. β-tubulin was used as a loading control.

Northern and Western Blot Analyses. A Northern blot containing mouse embryo RNAs was obtained from BD Clontech and hybridized to a MEKK4 cDNA probe. Immunoblot analyses were performed by using anti-MEKK4 (12), anti-phospho-JNK, and anti-MKK4 (Cell Signaling Technology, Beverly, MA), anti-actin (Santa Cruz Biotechnology), anti-β-tubulin (Sigma), and anti-GAPDH (Abcam). Secondary antibodies were detected by chemiluminescence (Pierce).

Whole-Mount *in Situ* Hybridization. Dissected embryos were fixed in 4% paraformaldehyde (PFA) in 0.1 M phosphate buffer, digested with proteinase K, fixed in PFA again, and then hybridized to digoxigenin-labeled probes (Roche Applied Science) at 70°C overnight. On the following day, embryos were washed and incubated with anti-digoxigenin-AP-Fab fragment (Roche Applied Science). Bound antibody was visualized by using BM purple-precipitating reagents (nitroblue tetrazolium/5-bromo-4-chloro-3-indolyl phosphate) as suggested by the manufacturer (Roche Applied Science).

Histology and Immunostaining. For preparation of semithin sections, E8.5-E10.5 embryos were processed in a fixative containing 4% PFA and 1.25% glutaraldehyde in 0.1 M phosphate buffer. Tissues were treated with 1% osmium, dehydrated, embedded in plastic, and semithin ($\approx$1 μm) sections were stained with 1% Toluidine blue. E18.5 embryo heads were fixed in Bouin's solution, embedded in paraffin, and 12- to 14-μm sections were stained with 0.1% thionin.

For immunostaining, E9.5 embryos were fixed for 1 h in 4% PFA at 4°C, rinsed in PBS, cryoprotected, and frozen over liquid N_2. Transverse sections (14 μm) of embryos were cut on a cryostat. For phospho-JNK immunostaining, sections were pretreated by boiling in an antigen unmasking solution (Vector Laboratories) in a microwave for 12 min before addition of the primary antibody. The following primary rabbit polyclonal antibodies were used: anti-phospho-MKK4 and anti-phospho-JNK (1:200; Cell Signaling Technology), and anti-phospho-histone H3 (1:1,000; Upstate Biotechnology, Lake Placid, NY). Sections were incubated with biotinylated goat anti-rabbit secondary antibody (1:200; Vector laboratories), then labeled with peroxidase (ABC kit, Vector Laboratories), and finally visualized by using a diaminobenzidine substrate kit (Vector Laboratories).

TUNEL Assays. For TUNEL assays, E8.5-E10.5 embryos were fixed for 1 h in 4% PFA, cryoprotected in sucrose, and frozen over liquid N_2. For brain sections, 14-μm transverse sections were processed in accordance with the manufacturer's instructions by using an ApopTag apoptosis detection kit (Serologicals, Clarkston, GA). Sections were counterstained with TO-PRO-3 iodide (1:1,000; Molecular Probes). E8.5 embryos used for whole-mount TUNEL analysis were pretreated by transferring the embryos into methanol, bleached for 5 h at 4°C in methanol/H_2O_2 (5:1), rinsed in PBS, and then processed by using the ApopTag kit accordingly. However, instead of using a Cy3-conjugated mouse monoclonal anti-digoxigenin antibody (1:100; Jackson ImmunoResearch) as in brain sections, a biotin-SP-conjugated mouse monoclonal anti-digoxigenin antibody was used (1:100; Jackson ImmunoResearch). Embryos were peroxidase-labeled (ABC kit, Vector Laboratories) and visualized by using a diaminobenzidine substrate kit (Vector Laboratories).

Quantification of Active MKK4 and JNK Immunoreactivity. For phospho-MKK4 and phospho-JNK immunoreactivity in the FB and HB regions, color images (300-dpi resolution) of immunostained sections were captured by using a Prog/Res/3012 camera (Kontron Elektronic) attached to a Zeiss Axiophot 2 microscope.

Table 1. Genotypic and phenotypic analyses of embryos derived from MEKK4 heterozygous crosses

	Genotype			Phenotype			
Stage	+/+	+/−	−/−	EX	EX plus SB	SB/CT	MEKK4−/− with NTD
E10.5	36	56	32 (26%)	22 −/−, 2 +/−	N/A	N/A	N/A
E14.5–15.5	8	21	11 (28%)	4 −/−, 1 +/−	3 −/−	2 −/−	82%
E17.5-perinatal	41	80	45 (27%)	15 −/−, 1 +/−	7 −/−	18 −/−, 1 +/−	89%

Embryos at various stages were dissected, examined, and genotyped. Percentages of MEKK4−/− embryos at each stage are shown in parentheses. EX, embryos showed exencephalic phenotype without spina bifida; EX plus SB, embryos showed exencephaly in combination with SB; SB/CT, embryos showed no obvious cranial phenotype but had SB and/or CT; N/A, spinal/tail defects in E10.5 embryos were not determined.

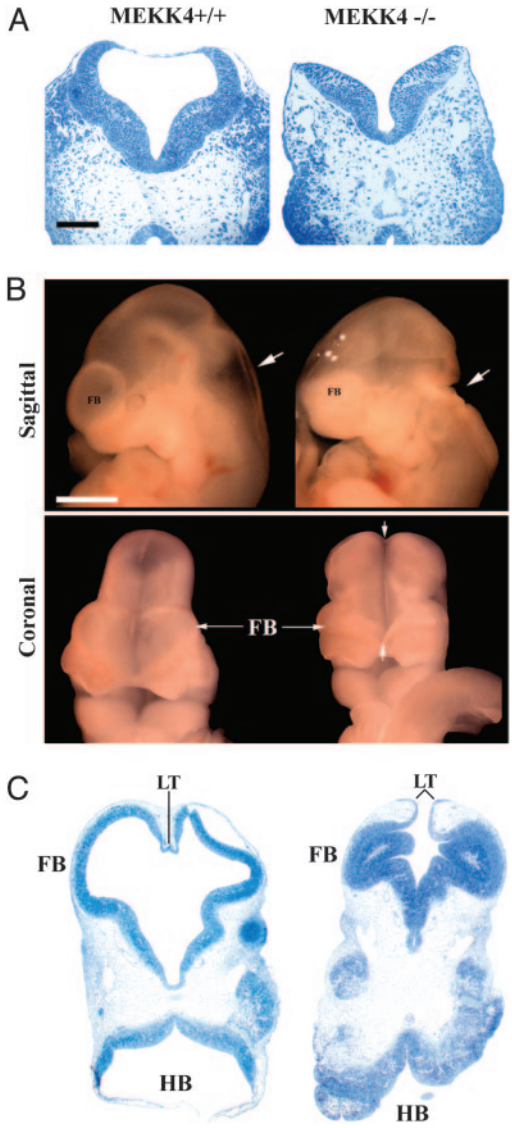

Fig. 2. Neural tube defects in MEKK4−/− mice. (*A*) Horizontal semithin sections of E9.5 HBs showed an open neural tube in MEKK4−/− embryos (*Right*), whereas the neural tube of wild-type littermates was closed (*Left*). (*B*) Sagittal and coronal views of E10.5 embryos showed failed fusion of the neural tube and structural defects spanning the HB (arrows in sagittal view) to the FB (arrows in coronal view). (*C*) Horizontal semithin sections at E10.5 showed failed neural tube closure at the LT and an open HB in MEKK4−/− mice (*Right*). The FB of MEKK4−/− embryos also had ventricular stenosis, yielding a more dense appearance of the FB (see sagittal view in *B*). (Bars, 100 μm in *A*; 1,000 μm in *B*.)

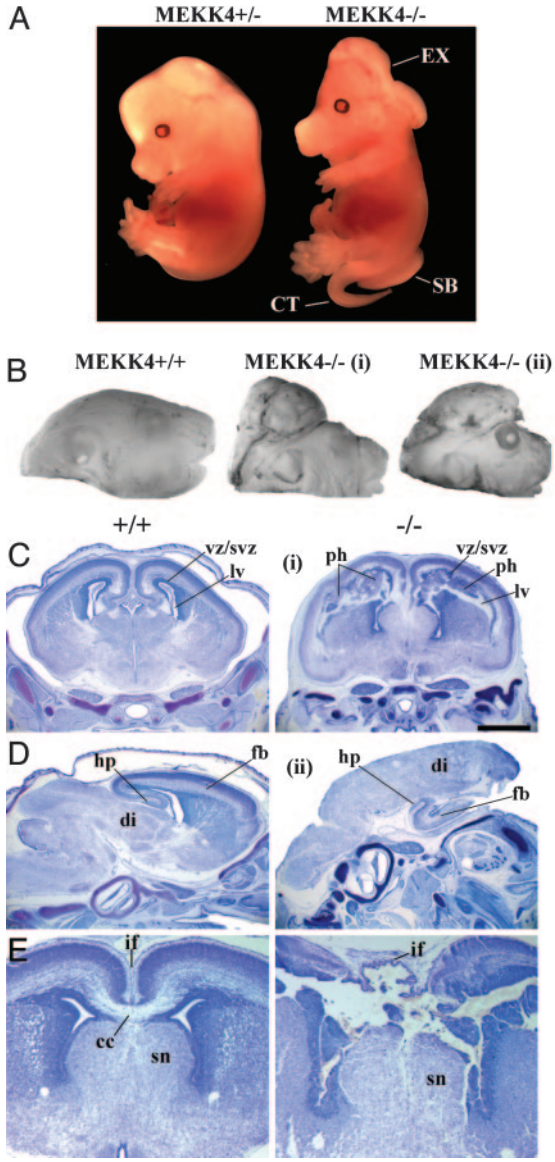

Fig. 3. Neural tube defects and brain malformations in later-stage MEKK4−/− embryos. (*A*) An E14.5 MEKK4−/− embryo (*Right*) displayed cranial EX, SB, and CT. (*B*) Pictures of a MEKK4+/+ (*Left*) and two MEKK4−/− (*i* and *ii*) E18.5 embryos. Both MEKK4−/− embryos developed EX, and MEKK4−/−(*ii*) embryos also showed exposed eyes. (*C* and *D*) Nissl-stained coronal (*C* and *E*) and sagittal (*D*) sections of E18.5 MEKK4+/+ (*Left*) and MEKK4−/− (*Right*) brains. MEKK4−/−(*i*) embryo had a relatively normal-sized FB but contained severely disrupted lateral ventricles (lv) and bilateral periventricular heterotopias (ph). These abnormal periventricular heterotopias structures disrupted continuities of the ventricular/subventricular zones (VZ/SVZ). In the MEKK4−/−(*ii*) embryo, the diencephalon (di) extended over the FB, which was small and rudimentary, but still possessed certain structures such as the hippocampus (hp). (*E*) At the level of the septal nucleus (sn), MEKK4−/−(*i*) FB showed severe morphological disruptions at the interhemispheric fissure (if) and corpus callosum (cc). (Bar,1 mm in *C*.)

Images were opened in PHOTOSHOP 7.0 (Adobe Systems, San Jose, CA) and converted to a 256 grayscale (with 0 being black and 256 being white). To analyze the intensity of staining at the rostral extremity of the HB neural folds, each fold had three 50-μm-diameter circles placed adjacently to one another, beginning at the most rostral edge and centered over the neuroepithelial layer (see bracketed region in Fig. 4*A*). Because FB neuroepithelium surrounding the lamina terminalis (LT) was thinner, three circles of 25 μm in diameter were placed on either side of the LT (see bracketed region in Fig. 4*A*) For each circle, a mean grayscale value was determined and thus a mean average for each tissue section. To control for inherent staining variability, we compared the intensity of staining relative to a background reference (averages of two 50-μm-diameter circles placed over cephalic mesenchyme/section in HB). There was no statistical difference between MEKK4+/+, MEKK4+/−, and MEKK4−/− mice in the intensity of background staining. We then subtracted the mean background value from mean HB or FB values and divided by the mean background. Because 0 corresponds to black in our grayscale, all values were multiplied by −100 so that positive percentage changes relative to background reflected an increase in staining, whereas negative values

Table 2. Effects of folic acid and inositol treatment on the incidence of NTD in MEKK4−/− embryos

Treatment	Total embryos	MEKK4−/− embryos	EX	EX plus SB	SB	Normal
PBS	56	11	3	3	3	2 (18%)
Folic acid	34	10	5	2	1	2 (20%)
Inositol	45	8	2	2	4	0 (0%)

a decrease in staining. For quantitation and statistical analysis, we used the following numbers of E9.5 embryos (total sections are in parentheses): phospho-MKK4 in HB: +/+, 6 (16) +/−, 4 (6) and −/−, 6 (18) phospho-MKK4 in FB: +/+, 4 (6) +/−, 3 (6) and −/−, 4 (7) phospho-JNK in HB: +/+, 6 (18) +/−, 2 (5) and −/−, 6 (24) and phospho-JNK in FB: +/+, 6 (13); +/−, 2 (3); and −/−, 6 (16).

Statistical Analysis. Group differences were compared between MEKK4+/+, MEKK4+/−, and MEKK4−/− mice by using ANOVA, with a P value of <0.05 being considered significant. All data were displayed as mean ± SEM.

Results

We have previously observed that on a mixed C57BL/6 × 129/SvE background, viable MEKK4−/− mice were obtained from MEKK4+/− crosses with a reduced Mendelian ratio (15%, rather than 25% of the progeny were MEKK4−/−) (12). When the MEKK4 mutation was backcrossed onto C57BL/6 background for more than five generations, no MEKK4−/− mice survived at weaning age. To investigate a role for MEKK4 in embryonic development, we analyzed the expression patterns of MEKK4. Northern blot analysis revealed that MEKK4 mRNA was expressed in all of the embryonic stages examined, from E7 to E17 (Fig. 1*A*). Whole-mount *in situ* hybridization showed widespread expression of MEKK4 mRNA in E9 embryos (Fig. 1*B*). Notably, MEKK4 expression was highest in the developing neural tube that includes prospective brain and spinal cord regions, suggesting a role for MEKK4 in neural development. Accordingly, MEKK4 protein was expressed in E10.5 heads and E18.5 brains of wild-type mice and absent in MEKK4−/− tissues (Fig. 1*C*).

To examine whether loss of MEKK4 affects a particular stage of embryonic development, we collected embryos derived from MEKK4+/− crosses at various stages (E9.5 to E18.5). MEKK4−/− embryos were found at close to Mendelian ratios at all fetal stages, indicating that MEKK4 is dispensable for survival of embryos (Table 1). However, we found that >80% of MEKK4−/− embryos developed NTDs (Table 1). The NTD phenotypes in these mice included cranial exencephaly (EX), spina bifida (SB), curled tail (CT), or any combination of these malformations (see below). Approximately 3% of MEKK4+/− mice also exhibited NTDs. The incidence of NTDs was similar between male and female MEKK4−/− embryos (data not shown). No obvious defects outside the nervous system could be identified in MEKK4−/− embryos. These mutants survived to birth but died shortly afterward.

Mutant MEKK4−/− embryos could be distinguished morphologically as early as E9.25–E9.5 because the cranial neural folds did not converge at the dorsal midline, resulting in an open neural tube (Figs. 2*A* and 4*A*). At E10.5, MEKK4−/− mice had failed neural tube closure, spanning from the LT in the anterior FB to the HB/spinal cord junction (Fig. 2 *B* and *C*). In addition, the ventricles of MEKK4−/− mice appeared constricted and filled with cells instead of ventricular space (Fig. 2*C*), which was probably due to collapse of the dorsal onto ventral neuroepithelium as a result of unfused FB vesicles. At E14.5, MEKK4−/− mice could display both EX and SB/CT (Fig. 3*A*). By E18.5, two typical brain phenotypes were observed in exencephalic MEKK4−/− embryos (Fig. 3 *B–E*). Approximately 30% (6 of 20 embryos) of MEKK4 mutants displayed FBs of similar size to wild-type but contained markedly deformed ventricles and periventricular heterotopias (Fig. 3 *C* and *E*) positive for both neuronal and proliferative cell markers (data not shown). Approximately 70% (14 of 20 embryos) of MEKK4 mutants had FBs that were smaller and/or rudimentary and had prominent diencephalic expansions overlying the remaining inverted cortex (Fig. 3*D*). The defects observed at the LT in E9.5 MEKK4−/− mice might be expected to cause impaired corpus callosum formation. Indeed, E18.5 MEKK4−/− embryos showed severe disruption of corpus callosum development (Fig. 3*E*). Given the expression patterns of MEKK4 (Fig. 1) and the early NTD phenotypes, it appears that MEKK4 has a critical role in facilitating closure of the neural tube along the entire neuraxis. Loss of this function in MEKK4−/− mice may yield variable CNS abnormalities and midline fusion failure at later stages, depending on the sites where the initial neural tube closure is affected.

Clinical trials have demonstrated that dietary supplementation of folic acid in early pregnancy can prevent up to 70% of NTDs (17). In addition, administration of inositol reduces the incidence of spinal NTDs in *curly tail*, a mouse model of folate-resistant NTDs (15). To evaluate whether NTDs in MEKK4−/− mice respond to such treatment, we administered these agents to pregnant dams according to established protocols (15, 16). Compared with control saline treatment, folate or inositol had no significant effects on the occurrence of NTDs in MEKK4−/− embryos (Table 2). Thus, MEKK4 deficiency affects a molecular pathway that is resistant to folate- and inositol-mediated rescue effects.

To determine the molecular mechanism of NTDs in MEKK4−/− embryos, we examined the expression and activity of molecules downstream of MEKK4. MKK4/SEK1 is a direct target of MEKK4 *in vitro* and serves as a signaling intermediate between MAP3K and JNK/p38 pathways (13, 18). Immunostaining for phospho-MKK4, the activated form of MKK4, in E9.5 wild-type embryos showed that the levels were enriched in cells lining the CNS ventricles, the rostral portions of the HB neural folds, and the anterior FB neuroepithelium surrounding the LT (Fig. 4*A*). In contrast, in MEKK4−/− embryos with cranial NTDs, the intensity of phospho-MKK4 staining was significantly reduced in both the HB and FB neuroepithelium (Fig. 4 *A* and *B*). The reduction of active MKK4 was not due to decreased MKK4 expression (Fig. 4*C*). MEKK4 is therefore required for MKK4 activation at sites of neural tube closure. The residual phospho-MKK4 staining in mutant embryos, for example, in cells lining the CNS ventricles, could result from MKK4 activation through alternative MAP3K pathways.

Dysregulated apoptosis is detrimental to neural tube closure (2). Using TUNEL assays, we found that at E8.5, MEKK4−/− embryos showed massively elevated cell death in the entire neuroepithelium (Fig. 5*A*). In addition, Toluidine blue staining of semithin sections revealed increased occurrence of pyknotic nuclei within the HB/midbrain neuroepithelium (Fig. 5*B*). Enhanced neuroepithelial apoptosis was also observed in E9.5 (Fig. 5*C*) and E10.5 embryos (data not shown). Thus, loss of MEKK4

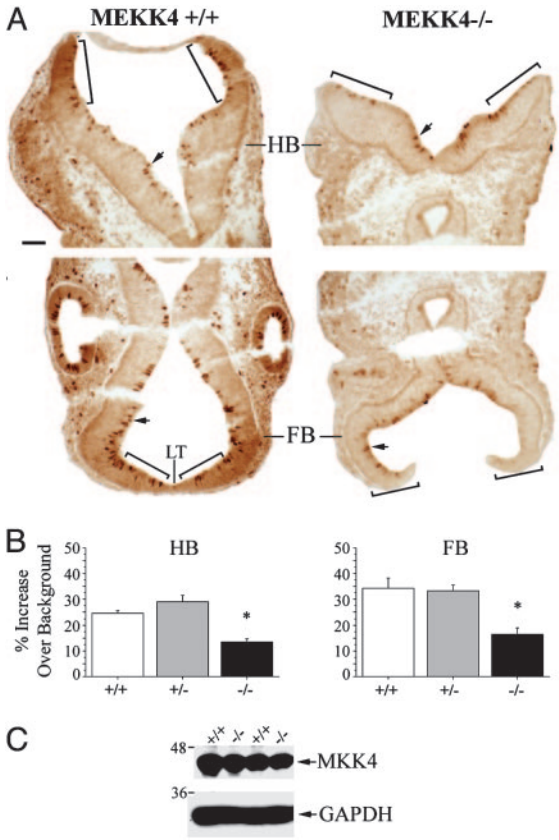

Fig. 4. Reduced active MKK4 during neural tube closure in MEKK4−/− mice. (*A*) Immunostaining for phospho-MKK4 at E9.5 in the HB (*Upper*) and FB (*Lower*). Wild-type mice (*Left*) had strong staining in the neuroepithelial layers of dorsal HB and FB surrounding the LT. MEKK4−/− mice (*Right*) showed reduced staining in these areas. Bracketed regions were areas analyzed for quantification in Fig. 3*B*. Enriched staining in cells lining the HB and FB ventricles (arrows) was observed in both genotypes. (*B*) Quantification (described in *Methods*) of phospho-MKK4 staining in the HB and FB. MEKK4−/− mice showed significant decreases in the intensity of staining in both the HB and FB neuroepithelium compared with MEKK4+/+ or MEKK4+/− mice. *, $P < 0.05$ (ANOVA). (*C*) Western blot for total MKK4 at E9.5 showed comparable levels between MEKK4+/+ and MEKK4−/− mice. GAPDH was used as a loading control. (Bar, 50 μm in *A*.)

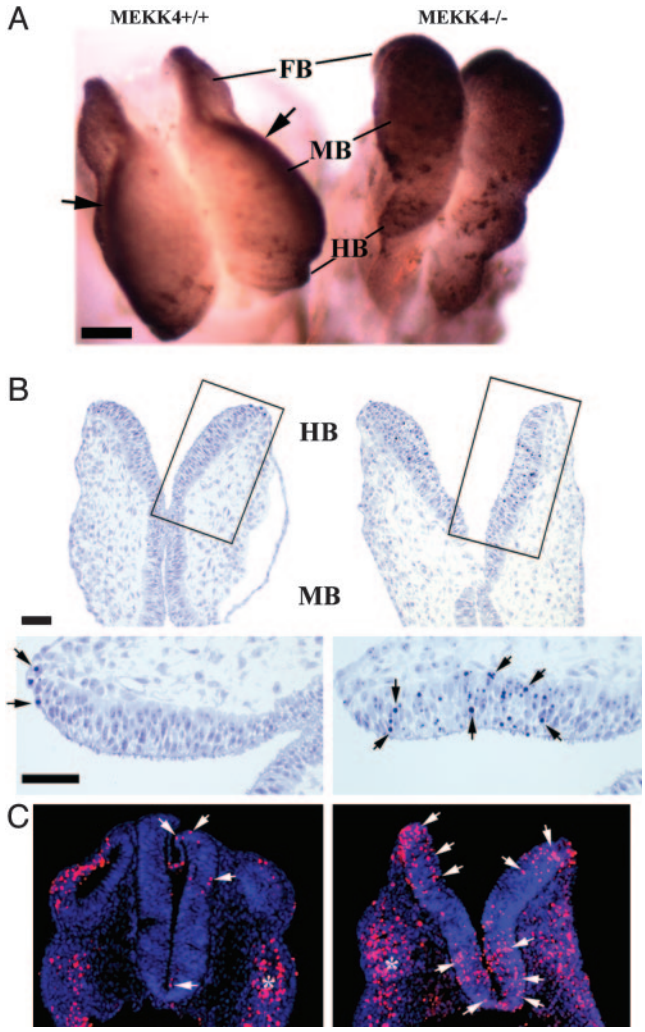

Fig. 5. Enhanced apoptotic cell death in MEKK4−/− neural tube. (*A*) Whole-mount TUNEL staining of E8.5 MEKK4+/+ (*Left*) and MEKK4−/− (*Right*) mice. In MEKK4+/+ mice, TUNEL-positive cells were largely restricted to the leading edges (arrows) of the cranial neural tube. In MEKK4−/− mice, TUNEL positivity was observed in the entire neural folds. (*B*) E8.5 horizontal semithin sections stained with Toluidine blue. Higher magnification of the boxed areas revealed limited pyknotic nuclei in MEKK4+/+ embryos (arrows), whereas MEKK4−/− embryos showed more numerous pyknotic nuclei throughout the neuroepithelium. (*C*) TUNEL staining of E9.5 embryos showed increased TUNEL-positive cells (red; arrows) in MEKK4−/− HB neuroepithelium (*Right*) compared with MEKK4+/+ (*Left*). Apoptosis was also observed in adjacent neural crest tissue (asterisks) in both genotypes. Sections were counterstained with TOPRO-3 for all nuclei (blue). (Bars, 100 μm in *A*; 50 μm in *B*.)

results in enhanced apoptosis before, during, and after neural tube closure periods. These observations strongly suggest that the excessive cell death is unlikely to be a consequence of failed neural tube closure, but rather, a direct event induced by MEKK4 deficiency that may contribute to development of NTDs. Taken together, our studies have revealed an antiapoptotic role of MEKK4 during development.

Altered cell proliferation in the neural tube has also been associated with NTDs (2). To compare the number of dividing cells in the HBs of E9.5 MEKK4+/+, MEKK4+/−, and MEKK4−/− embryos, we stained and quantified cells positive for phospho-histone H3, a marker of cells in M phase (Fig. 6, which is published as supporting information on the PNAS web site). The number of positive cells was normalized to the neuroepithelial area, which was found to be comparable between normal and mutant embryos. We did not find any dramatic change in the number of phospho-histone H3-positive cells relative to the neuroepithelial area between control (MEKK4+/+ and MEKK4+/−) and MEKK4−/− embryos. Therefore, loss of MEKK4 does not appear to have a major effect on proliferation in the neuroepithelium at the time of neural tube closure.

Discussion

We demonstrate that MEKK4 function is critical for neural tube closure. NTDs also result from deficiency in the MEKK4 upstream activator GADD45α (19, 20) and deletion of two downstream targets, JNK1 and JNK2 (10, 11). The increased apoptosis and degeneration in the FB of many MEKK4−/− mice is similar to that observed in JNK1/JNK2 double mutants. However, the enhanced HB apoptosis in MEKK4−/− embryos differs from JNK1/JNK2 mutants that show reduced HB apoptosis (10, 11). Thus, it appears unlikely that the antiapoptotic function of MEKK4 occurs entirely through JNK during neural tube closure. Accordingly, we did not detect alterations in JNK activity in E9.5 MEKK4−/− embryos by immunostaining and Western blot analyses (Fig. 7, which is published as supporting information on the PNAS web site). However, because the three

JNK proteins have distinct functions in various physiological processes (9), we cannot rule out the possibility that altered activity of one JNK isoform in MEKK4−/− mice is masked by compensatory changes of other isoforms. To identify potential downstream targets of MEKK4, we also examined phosphorylation of p38 and c-jun, expression of p53, and actin cytoskeletal organization, but observed no consistent changes in MEKK4−/− embryos (data not shown). Significantly, we found a marked reduction of MKK4 activity in the neuroepithelium of MEKK4−/− embryos. Like MEKK4, MKK4 has a crucial antiapoptotic function during embryonic development, although MKK4−/− mice are not reported to develop NTDs (21, 22). This result could be due to genetic redundancies of MAP kinase kinases downstream of MEKK4, or the influence of particular genetic backgrounds (note that NTDs in MEKK4−/− mice depend on genetic backgrounds). In any event, the finding that active-MKK4 is decreased as a result of MEKK4 deficiency provides strong evidence that MKK4 is a physiological target of MEKK4 *in vivo*.

NTDs remain prevalent birth defects despite folate supplementation in early pregnancy, indicating that the majority of the residual cases are folate-resistant (17). Because no human genes associated with NTDs have been identified, genetically modified mice are valuable systems to study NTDs (2, 3). However, current mouse models have two major limitations. First, unlike NTD patients that are usually nonsyndromic, most mutant mice show complex phenotypes involving other tissues that cause early embryonic lethality; the occurrence of NTDs may be secondary to abnormalities in other developmental systems. Second, very few models exhibit a genetic cosegregation of EX and SB as in NTD patients. Indeed, *curly tail* is considered the only mouse strain phenocopying the common human NTD (1). With features analogous to the human condition, MEKK4−/− mice represent a model for folate-resistant NTDs. Given the severe NTD phenotypes observed in the majority of MEKK4−/− and 3% of MEKK4+/− mice, MEKK4 is an important candidate gene for untreatable NTDs in human patients.

We thank J. Bao for technical assistance; J.H. Shim for advice on *in situ* hybridization; F. Manzo for manuscript preparation; and E. Ang, C. Bartley, J. Breunig, R.J. Davis, and Y.Y. Wan for helpful comments on the manuscript. This work was supported by a Child Health Research Grant from the Charles H. Hood Foundation, Inc. (Boston) (to H.C.), a James Hudson Brown–Alexander Brown Coxe Fellowship (to M.R.S.), a National Institute of Neurological Disorders and Stroke grant (to P.R.), and an American Heart Association grant (to P.R.). R.A.F. is an Investigator of the Howard Hughes Medical Institute.

1. Manning, S. M., Jennings, R. & Madsen, J. R. (2000) *Ment. Retard. Dev. Disabil. Res. Rev.* **6,** 6–14.
2. Copp, A. J., Greene, N. D. & Murdoch, J. N. (2003) *Nat. Rev. Genet.* **4,** 784–793.
3. Juriloff, D. M. & Harris, M. J. (2000) *Hum. Mol. Genet.* **9,** 993–1000.
4. Kuida, K., Haydar, T. F., Kuan, C. Y., Gu, Y., Taya, C., Karasuyama, H., Su, M. S., Rakic, P. & Flavell, R. A. (1998) *Cell* **94,** 325–337.
5. Hakem, R., Hakem, A., Duncan, G. S., Henderson, J. T., Woo, M., Soengas, M. S., Elia, A., de la Pompa, J. L., Kagi, D., Khoo, W., *et al.* (1998) *Cell* **94,** 339–352.
6. Phelan, S. A., Ito, M. & Loeken, M. R. (1997) *Diabetes* **46,** 1189–1197.
7. Pani, L., Horal, M. & Loeken, M. R. (2002) *Genes Dev.* **16,** 676–680.
8. Kyriakis, J. M. & Avruch, J. (2001) *Physiol. Rev.* **81,** 807–869.
9. Davis, R. J. (2000) *Cell* **103,** 239–252.
10. Kuan, C. Y., Yang, D. D., Samanta Roy, D. R., Davis, R. J., Rakic, P. & Flavell, R. A. (1999) *Neuron* **22,** 667–676.
11. Sabapathy, K., Jochum, W., Hochedlinger, K., Chang, L., Karin, M. & Wagner, E. F. (1999) *Mech. Dev.* **89,** 115–124.
12. Chi, H., Lu, B., Takekawa, M., Davis, R. J. & Flavell, R. A. (2004) *EMBO J.* **23,** 1576–1586.
13. Derijard, B., Raingeaud, J., Barrett, T., Wu, I. H., Han, J., Ulevitch, R. J. & Davis, R. J. (1995) *Science* **267,** 682–685.
14. Kaufman, M. H. (1995) *The Atlas of Mouse Development* (Academic, San Diego).
15. Greene, N. D. & Copp, A. J. (1997) *Nat. Med.* **3,** 60–66.
16. Gefrides, L. A., Bennett, G. D. & Finnell, R. H. (2002) *Teratology* **65,** 63–69.
17. MRC Vitamin Study Research Group (1991) *Lancet* **338,** 131–137.
18. Gerwins, P., Blank, J. L. & Johnson, G. L. (1997) *J. Biol. Chem.* **272,** 8288–8295.
19. Takekawa, M. & Saito, H. (1998) *Cell* **95,** 521–530.
20. Hollander, M. C., Sheikh, M. S., Bulavin, D. V., Lundgren, K., Augeri-Henmueller, L., Shehee, R., Molinaro, T. A., Kim, K. E., Tolosa, E., Ashwell, J. D., *et al.* (1999) *Nat. Genet.* **23,** 176–184.
21. Ganiatsas, S., Kwee, L., Fujiwara, Y., Perkins, A., Ikeda, T., Labow, M. A. & Zon, L. I. (1998) *Proc. Natl. Acad. Sci. USA* **95,** 6881–6886.
22. Nishina, H., Vaz, C., Billia, P., Nghiem, M., Sasaki, T., De la Pompa, J. L., Furlonger, K., Paige, C., Hui, C., Fischer, K. D., *et al.* (1999) *Development (Cambridge, U.K.)* **126,** 505–516.